Functional local connections with differential activity-dependence and critical periods surrounding the primary auditory cortex in rat cerebral slices

Ryuichi Hishida,* Daiki Kamatani, Hiroki Kitaura, Masaharu Kudoh, and Katsuei Shibuki

Department of Neurophysiology, Brain Research Institute, Niigata University, 1 Asahi-machi, Niigata 951-8585, Japan

Sensory information is processed in neural networks connecting the primary sensory cortices with surrounding higher areas. Here, we investigated the properties of local connections between the primary auditory cortex (area 41) and surrounding areas (areas 20, 36, 18a and 39) in rat cerebral slices. Neural activities elicited by repetitive electrical stimulation were visualized using the activity-dependent changes in endogenous fluorescence derived from mitochondrial flavoproteins, which mostly reflect activities produced by polysynaptic glutamatergic transmission. Polysynaptic feedforward propagation was dominant compared with the corresponding polysynaptic feedback propagation between the primary (area 41) and secondary (areas 20 and 36) auditory cortices, while such a tendency was less clear in other pathways. Long inter-areal (>1 mm) propagation with the same dominancy was observed after layer V stimulation between areas 41 and 20, and was not affected by cutting the underlying white matter. Activity-dependent changes in neural activities induced by low-frequency stimulation in the presence of 1 μM bicuculline were investigated using Ca^{2+} imaging. Significant potentiation of the polysynaptic Ca^{2+} activities was only observed in polysynaptic feedforward pathways from the primary to secondary auditory cortices. Experience-dependence of the connections between areas 41 and 20 was investigated using flavoprotein fluorescence imaging. The activities from areas 41 to 20 were reduced by cochlear lesions produced at P12 but not at P28, while the activities from areas 20 to 41 were reduced by the lesions at P28, suggesting the critical period for the polysynaptic feedforward connection was before P28, while for the polysynaptic feedback connection was after P28.
© 2006 Elsevier Inc. All rights reserved.

Introduction

Sensory information is serially processed in neural networks that involve the primary sensory cortices and surrounding and higher areas (Saper et al., 2000). These areas are mutually connected (Krieg, 1947; Bai et al., 2004), and neural activities recorded *in vivo* are formed by intimate interactions among the neural networks. For example, primary sensory cortices in the human brain can be activated by higher inputs during memory recall or imagery (Calvert et al., 1997; Halpern and Zatorre, 1999; Kosslyn et al., 1999), suggesting that not only feedforward connections from primary areas to higher areas but also feedback projections from higher areas to primary areas have important physiological roles. The properties of the feedforward and feedback projections have been extensively studied, especially in the visual cortex (Johnson and Burkhalter, 1996, 1997; Dong et al., 2004a,b). Some of these connections are composed of lateral axon collaterals of pyramidal neurons, and convey information directly through the areal boundary between cortical areas (Hofstetter and Ehret, 1992; Coogan and Burkhalter, 1993). Therefore, functional connections between different cortical areas are important, in addition to those within a particular cortical area.

Auditory information is processed by the primary auditory cortex and surrounding higher areas, such as language-related areas in humans (Dronkers et al., 2000). In the rat cerebral cortex, auditory-evoked potentials are recorded not only in the primary auditory cortex (area 41; Krieg, 1946a,b) but also in the adjacent areas (Barth et al., 1995). The primary auditory cortex is surrounded by ventral area 20 and caudal area 36, which have been identified as the secondary auditory cortices. Dorsal area 18a and rostral area 39 have been identified as the secondary visual and somatosensory cortices, respectively, which may function for multisensory integration (Barth et al., 1995; Brett-Green et al., 2003, 2004). The primary auditory cortex is connected to the surrounding areas through the areal boundaries. The functional connections between the primary and secondary auditory cortices may be more developed than those between the primary auditory cortex and the multisensory areas. The aim of the present study is to elucidate the properties of dynamic activity propagation in the polysynaptic neural networks at the areal boundaries around the primary auditory cortex, and we performed neural imaging in cortical slices for this purpose.

In our previous study, we found activity-dependent potentiation of polysynaptic activities between the primary auditory cortex and

---

* Corresponding author. Fax: +81 25 227 0814.
E-mail address: rhishida@bri.niigata-u.ac.jp (R. Hishida).
Available online on ScienceDirect (www.sciencedirect.com).

dorsal area 18a in cerebral slices perfused with bicuculline, an antagonist of $GABA_A$ receptors, using Ca^{2+} imaging (Hishida et al., 2003). This potentiation is likely to reflect some aspects of the functional connections, but could also be contaminated by an artifact caused by bicuculline or the Ca^{2+} indicator loaded into the slices. Recently, activity-dependent changes in endogenous flavoproteins have been applied to functional brain imaging *in vivo* (Shibuki et al., 2003; Reinert et al., 2004; Murakami et al., 2004; Coutinho et al., 2004; Weber et al., 2004; Shibuki et al., 2006, in press; Takahashi et al., 2006). This method allows us to measure polysynaptic neural activities without using exogenous indicators or $GABA_A$ antagonists in cerebral slices. In the present study, we investigated the properties of the functional connections surrounding the primary auditory cortex using flavoprotein fluorescence imaging and Ca^{2+} imaging. Our results suggest that polysynaptic feedforward connections from the primary to secondary auditory cortices allow efficient activity propagation, probably reflecting their importance in serial auditory information processing.

Materials and methods

Slice preparations

The experiments in this study were performed according to the guidelines of Niigata University. Wistar rats of both genders (6–9 weeks of age) were used. After being deeply anesthetized with ether, the rats were immersed in ice-cold water, except for the nose, for 3 min to reduce the brain temperature. Immediately after decapitation, a block of brain tissue including the left primary auditory cortex and surrounding cortices was dissected. The location of the primary auditory cortex was determined as area 41 of the temporal cortex (Krieg, 1946a,b), or Te1 of the temporal cortex (Zilles and Wree, 1985). Previously, we have reported that myeloarchitecture can be observed in a fresh slices because of light-scattering properties of myelinated fibers (Hishida et al., 2003). Thus identified cortical areas are generally well correlated to those in a classical map developed by Krieg, since fine differences in myeloarchitecture were used for identification of cortical areas in this classical map. Areas 20, 36, 18a and 39 (Krieg, 1946a,b; Cipolloni and Peters, 1979) were determined as the ventral, caudal, dorsal and rostral cortical areas adjacent to area 41, respectively (Fig. 1A). Slices (500 μm thick) including both area 41 and one of the surrounding areas were prepared from a cortical block in an ice-cold medium using a microslicer (DTK-2000; Dosaka, Osaka, Japan). Only one slice was selected from a number of slices prepared from a brain. The slice including areas 41 and 20 was prepared from the coronal plane at Bregma about −4.5 mm (judged from the unique shape of hippocampus in the cross-section surface). The slice including areas 41 and 36 was prepared from the horizontal plane at 2.0 mm dorsal from the dorsal edge of rhinal sulcus. The slices including areas 41 and 39 was prepared from the horizontal plane at 2.7 mm dorsal from the dorsal edge of rhinal sulcus. The slices including areas 41 and 18a was prepared as follows. We prepared 2–3 slices from the slanted coronal plane (at 60° to the horizontal plane) which passed through near the center of area 41 (judged from the slight bulge on the temporal cortical surface). Among these slices, the areal boundary between areas 41 and 18a was clearly observed in only one, and this slice was selected for further analyses. The position of the slices with regard to the borders of the cortical areas was confirmed in the translucent images of a fresh slice illuminated by near vertical light, since the contrast patterns of the images were very

similar to the myeloarchitecture because of the light scattering properties of the myelinated fibers (Hishida et al., 2003).We identified areas in the slices by comparing the contrast patterns with known myeloarchitecture in each area (Krieg, 1946a; Zilles and Wree, 1985). Estimated from the comparison between the contrast patterns of the image of a fresh slice and those of the myeloarchitecture stained in the fixed sections obtained from the same slice (Hishida et al., 2003), the areal boundaries could be determined with an accuracy of about 50 μm. If the boundary was not clearly observed, the slice was discarded. Each area was identifies as follow. Area 20 was identified as the ventral area adjacent to area 41 which had less myelinated fibers in layer IV than area 41 and had more myelinated fibers in layer V than the more ventral area. Area 36 was identified as the caudal area adjacent to area 41 which had less myelinated fibers in layers IV and V than area 41 and had more myelinated fibers in layer V than the more caudal area. Area 39 was identified as the rostral area adjacent to area 41 which had slightly less myelinated fibers in layer IV than area 41 and the more rostral area. Area 18a was identified as the dorsal area adjacent to area 41 which had less myelinated fibers in layers IV and V than area 41 and the more dorsal area. The composition of the medium was (in mM): NaCl 124, KCl 5, NaH_2PO_4 1.24, $MgSO_4$ 1.3, $CaCl_2$ 2.4, $NaHCO_3$ 26 and glucose 10. The medium was continuously bubbled with 95% O_2 and 5% CO_2 for at least 1 h before use. The slices were incubated for more than 1 h before recording. The recordings were performed at 25 ± 0.5°C.

Flavoprotein fluorescence imaging

Activity-dependent changes in endogenous flavoprotein fluorescence were used to visualize the polysynaptic neural activities elicited by repetitive stimulation of the slices (Shibuki et al., 2003). Each slice was placed in a recording chamber perfused with the above-described medium at a flow rate of 1 ml/min (Fig. 1B, inset). The surface of the medium in the chamber was covered with 95% O_2 and 5% CO_2 to prevent the escape of O_2 from the medium. In the chamber, the slice was placed on a membrane filter (H100A; Advantec, Tokyo, Japan). This hydrophilic polytetrafluoroethylene filter is permeable to oxygenated perfusion medium, and becomes transparent in the medium (Hishida et al., 2003; Shibuki et al., 2003). Areas and layers in the slice were identified based on the light-scattering patterns of the myelinated fibers observable in the translucent images (Hishida et al., 2003). In some experiments, the white matter under the areal boundary in the slice was cut by lowering a piece of razor blade attached to a manipulator down to the bottom of the recording chamber through the slice, and maintaining its position for a few minutes (Hishida et al., 2003). Endogenous green fluorescence ($\lambda = 520$–560 nm) of the slices in blue light (470–490 nm) was observed using an inverted epifluorescence microscope (TE300; Nikon; Fig. 1B) and an objective lens (magnification: 2.0; numerical aperture: 0.1). Images of the endogenous green fluorescence (123×164 pixels after binning; 31.4 μm/pixel) were recorded using a cooled CCD camera system (ARGUS/HiSCA; Hamamatsu Photonics, Hamamatsu, Japan) at 2 frames/s. By using a shutter the slices were exposed with the blue light only when the images were recorded. A total of 40 serial images were taken before and after repetitive stimulation in one trial, and the results recorded in 5 trials repeated at 2 min intervals were averaged. The slices were stimulated via Teflon-coated platinum wire (metal diameter: 50 or 125 μm). The cut end of the wire was placed on the surface of the slices, and biphasic current pulses (intensity: ±100 or 200 μA;
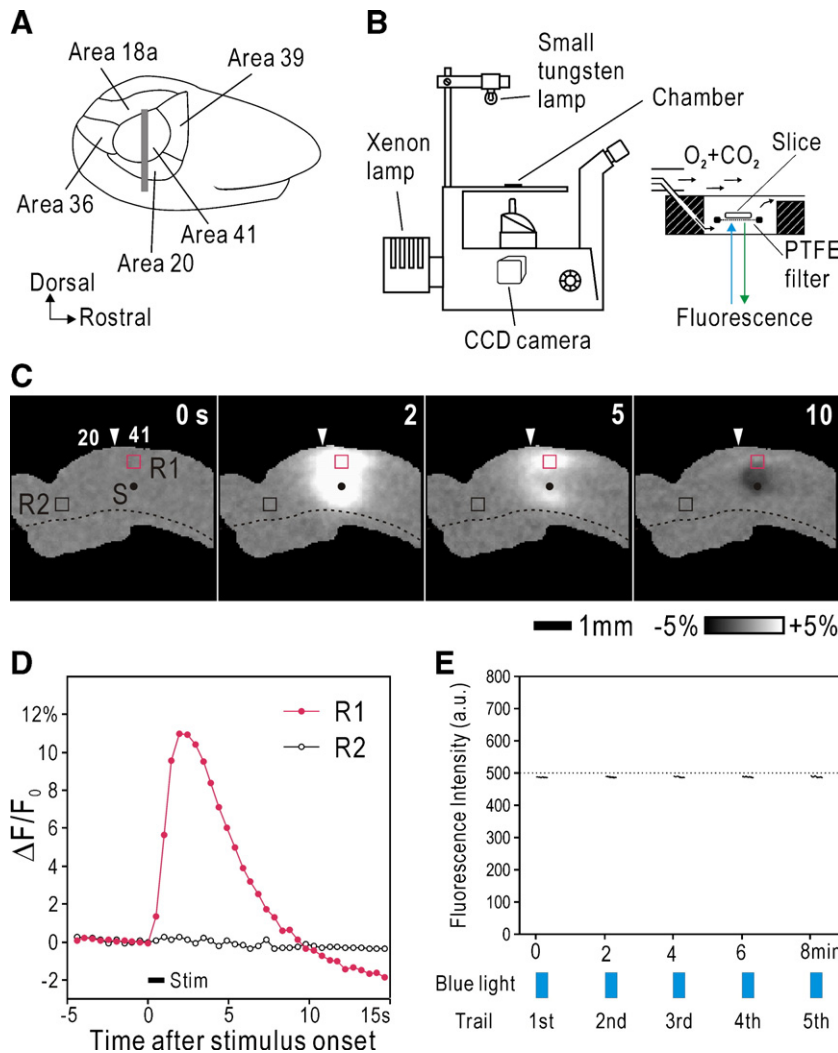
Fig. 1. Flavoprotein fluorescence imaging in cerebral slices. (A) Lateral view of the left side of the rat cerebral cortex. The positions of the primary auditory cortex (area 41) and surrounding areas are shown. The gray bar indicates the location of the slice which was used in th experiment of this figure. (B) Schematic drawing of the experimental setup. The inset shows the recording chamber. (C) Grayscale images of the changes in endogenous fluorescence intensity ($\Delta F/F_0$) elicited by repetitive electrical stimulation (200 µA, 10 Hz for 1 s) of layer V (S and black dots). The white arrowheads indicate the areal boundary between areas 41 and 20. The dotted lines show the boundary between the gray matter and the white matter. The time after the stimulus onset is shown in each image. (D) Time courses of the fluorescence changes recorded in the windows (squares) R1 and R2 in panel C. The horizontal bar represents the stimulus time. (E) Time courses of the fluorescence intensity recorded in the window R2 in panel C. The blue boxes indicate the time periods during which the slice was exposed with the blue excitation light. The dotted line shows the level of 500 (fluorescence intensity arbitrary units). (For interpretation of the references to colour in this figure legend, the reader is referred to the web version of this article.)

duration of each phase: 200 µs) at 10 or 20 Hz for 1 s were used for stimulation. Consecutive images were divided by the average of 10 images recorded immediately before the stimulation pixel-by-pixel for normalization, and the changes in fluorescence intensity ($\Delta F/F_0$) were estimated. The maximal amplitudes of flavoprotein fluorescence responses following stimulation (100 µA, 10 Hz for 1 s) were >5% in most slices. If this criterion was not satisfied, we discarded the slice. The fluorescence responses were stably recorded for more than 4 h from the beginning of the recordings (Shibuki et al., 2003). We finished the recording experiments within 3 h.

Ca²⁺ imaging

We also used Ca^{2+} imaging to investigate the polysynaptic neural activities. Rhod-2 was used as a Ca^{2+} indicator (Minta et al.,

1989), since it does not prevent synaptic potentiation in the primary auditory cortex (Seki et al., 1999, 2001; Kitaura et al., 2004) or potentiation of the polysynaptic activities between cortical areas (Hishida et al., 2003). For loading with rhod-2, slices were incubated in the above-described medium containing 10 µM rhod-2 tetraacetoxymethyl ester (rhod-2/AM), which was solubilized in 0.1% dimethyl sulfoxide and 0.1% Cremophore EL (polyoxyethylated castor oil), at room temperature for 1 h. The slices were rinsed with normal medium for at least 30 min before Ca^{2+} imaging. Each slice was set in the chamber as described for the flavoprotein imaging. The fluorescent Ca^{2+} images were recorded with an excitation wavelength of 546 ± 5 nm and an emission wavelength of >590 nm using the same ARGUS/HiSCA system. A total of 40 images (61×82 pixels; 63.4 µm/pixel) were sequentially recorded at intervals of 21 ms, and divided by the average of 10 images

collected before the stimulation for normalization. The maximal amplitudes of the Ca^{2+} signals elicited by a single pulse at 100 μA in the presence of 1 μM bicuculline were >10% in most slices. If this criterion was not satisfied, we discarded the slice. The amplitudes of Ca^{2+} responses were gradually decreased. Therefore, we finished the recording experiments within 1 h. To keep the distances between the recording and stimulation sites constant, the stimulation/recoding sites were located 2 mm apart from the boundaries in area 41 and 500 μm in other areas.

Deafferentation from cochlear inputs

Rats were deafened by cochleotomy at the ages of P10–12 or P28. Bilateral cochlear lesions were created using a retroauricular approach (Illing et al., 1999). The rats were anesthetized with fluothane (1.5% in O$_2$ gas), and the surgical operation was conducted under sterilized conditions. After local application of a local anesthetic, bupivacaine, the bulla tympani was opened. After visual identification of the cochlea, its whole structure was destroyed with a diamond drill head or the tip of a pair of forceps. Next, the bulla was filled with a small wad of sterile absorbent cotton or antibiotic ointment, and the wound was surgically closed. The function of the cochleae was also destroyed by streptomycin (Schaeppi et al., 1991), which was injected into the rats every day from P10 to P28 (400 mg/kg, i.p.). Hearing loss was confirmed by observing a loss of startle responses to hand clapping in the animals. Slices were prepared from the deafened rats at 7 weeks of age or later.

Data analysis

The mean and S.E.M. were calculated and shown in the figures. The numbers n or the numbers in the parentheses represent the numbers of slices used for the experiment. Statistical significance in the results was tested using a computer program (StatView, SAS Institute Inc., Cary, U.S.A.). Differences in the mean values of bar graphs were evaluated with the Mann–Whitney U-test, and only significant differences ($P < 0.05$) were labeled.

Drugs

6-Cyano-7-nitroquinoxaline-2,3-dione (CNQX, an antagonist of non-NMDA glutamate receptors) was purchased from Tocris Cookson (Bristol, UK). Rhod-2/AM was obtained from Dojindo Laboratories (Kumamoto, Japan). Bicuculline and Cremophore EL were purchased from Sigma. Bicuculline and CNQX were applied to the slices by addition to the perfusion medium. Streptomycin sulfate was purchased from Meiji Seika (Tokyo, Japan).

Results

Neural activities in cerebral slices visualized by using flavoprotein fluorescence imaging method

Neural activities in slices including the primary auditory cortex (area 41) were observed using flavoprotein fluorescence imaging. Repetitive stimulations at 10 Hz for 1 s were applied to layer V (Fig. 1C, black dots). Increases in the fluorescence intensity were observed around the stimulation site and in upper layer II/III, in which the neural activities spread laterally (Fig. 1C). The amplitude of the fluorescence increase ($\Delta F/F_0$) in a window of 10×10 pixels

placed in layer II/III reached a peak (>10%) at 2 s after the stimulus onset (Fig. 1D). The fluorescence signals in regions distant from the stimulation site remained stable (Fig. 1D). The fluorescence changes returned to the baseline level at about 10 s after the stimulus onset, and negative changes were observed for about 50 s (data not shown). To estimate the extent of bleaching and phototoxicity of the blue excitation light we used, the fluorescence intensity was measured from the start to the end of the above experiment (Fig. 1E). The fluorescence intensity was almost the same level during the 5 trials, suggesting that the bleaching and phototoxicity did not matter under the conditions of this study.

Directionally-different activity propagations between the primary auditory cortex and surrounding areas

We observed the activity propagation around the areal boundary using flavoprotein fluorescence imaging. First, we prepared slices containing the primary auditory cortex (area 41) and ventral area 20 (Fig. 2A). These areas and the boundary were easily distinguished by the well-developed thalamocortical fibers present in area 41, but absent from area 20, in a translucent image of each fresh slice (Fig. 2B; Hishida et al., 2003). A stimulating electrode was placed on a site in layer V at 500 μm from the boundary, and windows were placed in layer II/III of the other area adjacent to the boundary. Stimulation of area 41 produced laterally spreading activities in layer II/III. The elicited activities in layer II/III propagated not only toward area 20 but also to the opposite direction, forming a mushroom-shaped distribution of neural activities (Fig. 2C). Some parts of these activities invaded area 20, in which the signal amplitude in layer II/III reached 5.4±0.6% (mean±S.E.M., $n=6$). Stimulation of area 20 also caused spreading activities. Most of the strong activities were within area 20 (Fig. 2D), but a little amount of weak activities invaded area 41, in which the signal amplitude in layer II/III was only 2.1±0.2% ($n=6$). The amplitude of the signals propagating from the primary auditory cortex to area 20 was significantly larger than that of signals in the reverse direction ($P < 0.01$, Mann–Whitney U-test; Fig. 2E).

Next, we observed the activity propagation in other boundaries surrounding the primary auditory cortex (Fig. 3A). In slices containing caudal area 36, stimulation of layer V of area 41 produced a mushroom-shaped distribution of neural activities, while stimulation of area 36 produced skewed distribution of neural activities (Figs. 3Ac, d). These patterns were similar to those in the slices containing areas 41 and 20 (Figs. 3Aa, b). The signal amplitude of the activities from the primary auditory cortex to area 36 (7.0±0.8%, $n=6$) was significantly larger than that of the activities in the reverse direction (3.0±0.3%, $P < 0.01$; Fig. 3B). The directionally-different propagations between area 41 and the surrounding area were also observed in slices containing dorsal area 18a (Figs. 3Ae, f, Fig. 3B). The signal amplitude of the activities propagating from the primary auditory cortex to area 18a (4.4±0.5%, $n=7$) was slightly, but significantly, larger than that of the activities in the reverse direction (2.8±0.2%, $P < 0.01$; Fig. 3B). In slices containing rostral area 39, however, activity propagation between the areas was less clear than that between the primary and secondary auditory cortices (Figs. 3Ag, h, Fig. 3B), and the signal amplitude of the activities from area 41 to area 39 (2.3±0.1%, $n=10$) was slightly, but significantly, smaller than that of the activities in the reverse direction (3.1±0.2%, $P < 0.01$; Fig. 3B). When layer II/III was stimulated instead of layer V, a significant difference of activity propagations was only observed between
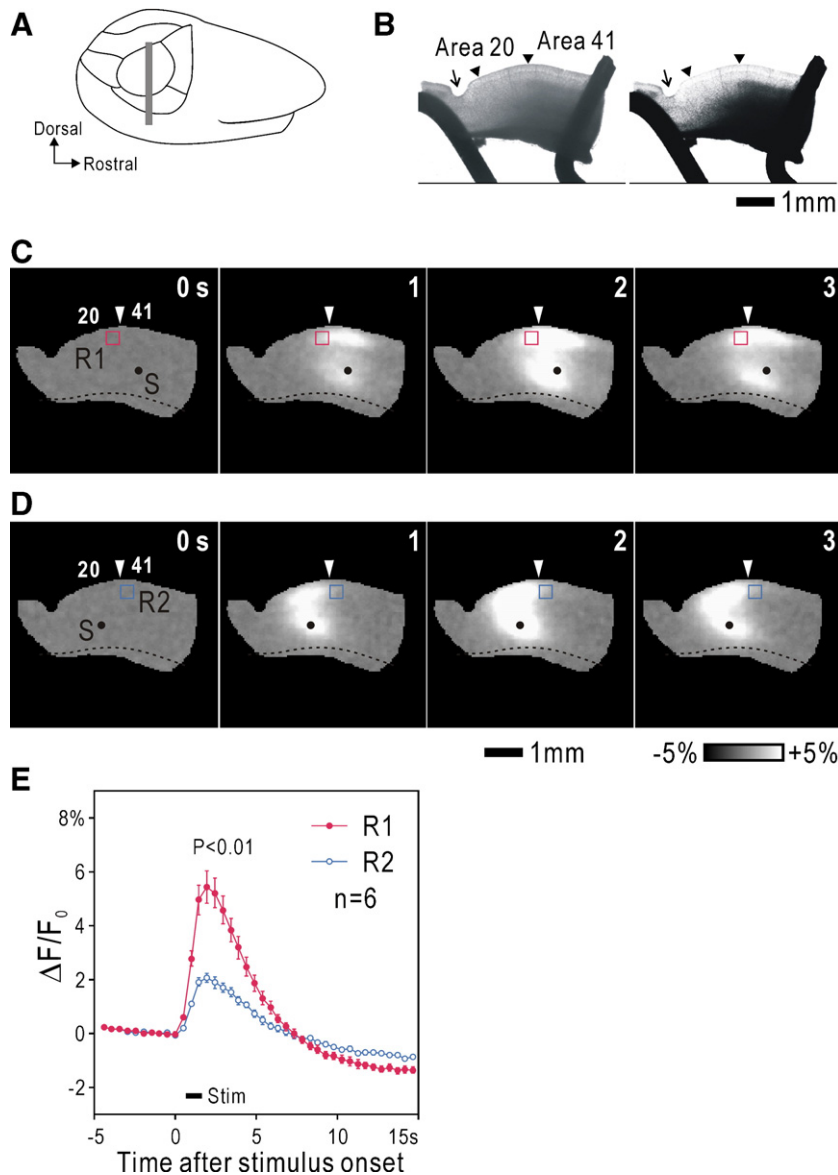
Fig. 2. Directionally-different activity propagations between the primary auditory cortex and ventral area 20. (A) Slice preparation. The gray bar indicates the location of the slice including ventral area 20. (B) Translucent image of a slice (left) and its contrast-enhanced image (right). Areas 41 and 20 can be identified by the difference in the light scattering patterns of layer IV. The black arrowheads indicate the dorsal and ventral boundaries of area 20. The arrow shows the rhinal sulcus. (C, D) Flavoprotein fluorescence responses following stimulation (200 μA, 20 Hz for 1 s) of layer V. The stimulated sites (S and black dots) are located in area 41 (C) or 20 (D) at a distance of 500 μm from the areal boundary (white arrowheads). The dotted lines show the boundary between the gray matter and the white matter. (E) Time courses of the fluorescence changes. The recording windows (squares), shown as R1 in panel C and R2 in panel D, were placed in layer II/III adjacent to the boundary. The signals recorded in two different experiments are superimposed.

areas 41 and 36 ($P<0.01$; Fig. 3C). Taken together, these results suggest that activity propagation from the primary to secondary auditory cortices is more dominant than that in the reverse direction, while no consistent tendency was observed between the primary auditory cortex and non-auditory surrounding areas.

Pyramidal neurons extend lateral axon collaterals for more than 1 mm (Gilbert, 1992), and their functions are important for sensory information processing (Das and Gilbert, 1995). Although in the Gilbert's review these lateral axon collaterals (horizontal connections) refer to the connections that are intrinsic to an area and do not refer to the connections between areas, we guessed that there may be also similar lateral axon collaterals for more than 1 mm between different cortical areas and neural activities may propagate

via the inter-areal lateral connections. To test this possibility, we applied layer V stimulation at sites about 1 mm from the areal boundary between the primary auditory cortex and ventral area 20. When the primary auditory cortex was stimulated, weak but distinct activities were observed in a column-like region including layers II/III and V in area 20 (Fig. 4A). The signal amplitude in a circular window (diameter: 20 pixels) placed in layer II/III was $1.8\pm0.2\%$ ($n=5$). On the other hand, almost no activity was observed in the corresponding region of area 41 when area 20 was stimulated (Fig. 4B), and the signal amplitude ($0.7\pm0.1\%$) was significantly smaller than that in the reverse direction (Fig. 4C). The peak amplitude appeared at about 2.5 s after the stimulus onset (Fig. 4C). Long inter-areal activity propagation was most effectively
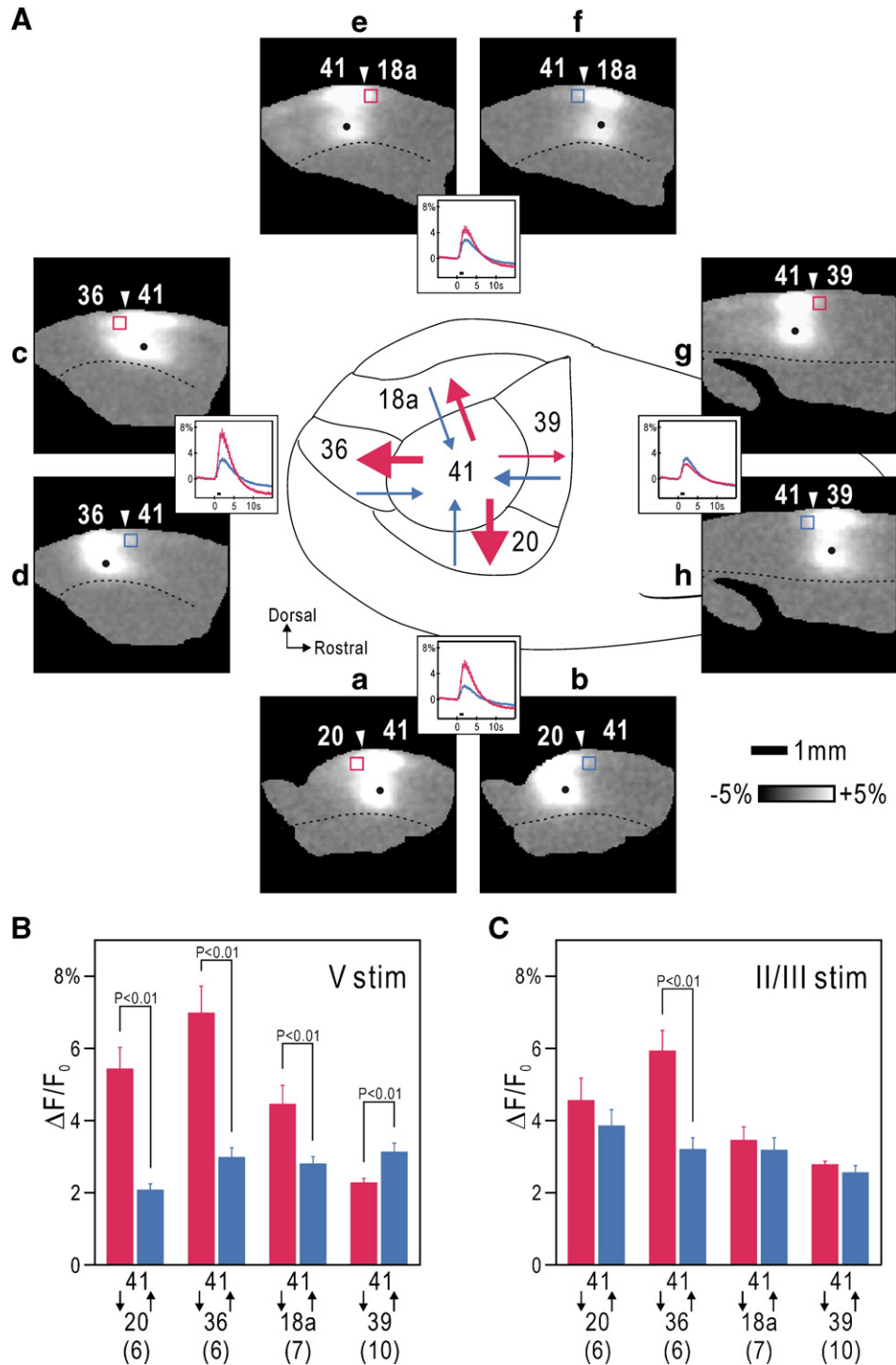
Fig. 3. Activity propagation between the primary auditory cortex and surrounding areas. (A) Flavoprotein fluorescence responses elicited by repetitive stimulation (200 μA, 20 Hz for 1 s) of layer V in various areas of slices including the primary auditory cortex and one of the surrounding areas. The insets show time courses of the fluorescence changes of each slice which were plotted the same as Fig. 2E. In the center schematic drawing, the sizes of the arrows give a rough impression of the magnitudes of the activity propagation via the areal boundaries. (B, C) Comparisons of the amplitudes of the activity propagation. The responses were evaluated at 2 s after the stimulus onset in the windows (squares) shown in panel A. Stimulation was applied to layer V (B) or layer II/III (C). (For further description, see legend to Fig. 2.)

produced by stimulation of layer V in area 41, while stimulation of other layers was significantly less effective ($P < 0.02$; Fig. 4D). Although a part of the stimulus current might leak to the nearby layers, layer-specificity of stimulus effects was confirmed by this

result. In these experiments, activity propagation was almost completely abolished by 10 μM CNQX, an antagonist of non-NMDA glutamate receptors ($n = 8$; Fig. 4E), indicating that the long inter-areal propagations were mediated by glutamatergic
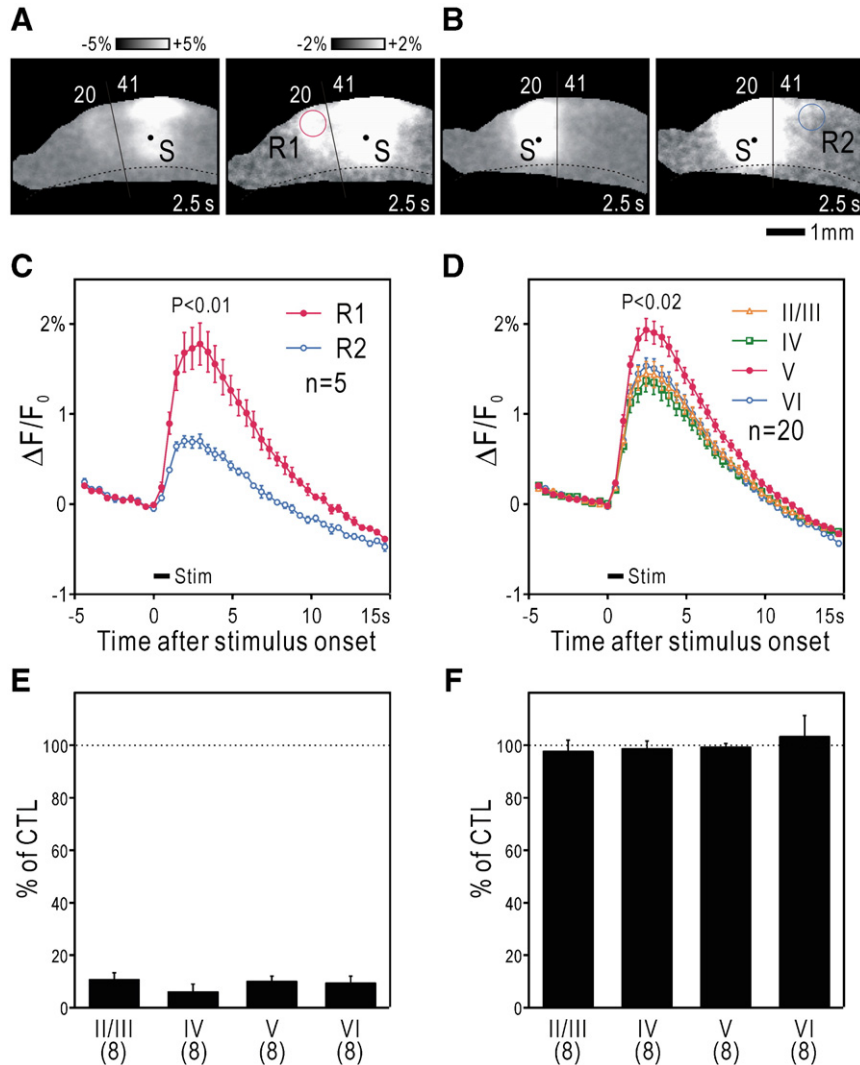
Fig. 4. Long inter-areal activity propagation between the primary auditory cortex and ventral area 20. (A) Flavoprotein fluorescence responses elicited by repetitive stimulation (100 μA, 10 Hz for 1 s) of layer V in the middle of area 41 (S and black dots). The black lines show the areal boundary. Note the left and right images are shown in different gray scales (−5% to +5% and −2% to +2%, respectively). In the right images, weak activities are emphasized. (B) Responses following repetitive stimulation of layer V in area 20 (500 μm from the boundary) of the same slice in panel A. (C) Time courses of the fluorescence changes in the circular windows in panels A (R1) and B (R2). A significant difference is found between the amplitudes at 2.5 s after the stimulus onset. (D) Time courses of the fluorescence changes in layer II/III of area 20 elicited by stimulation of layers II/III, IV, V or VI in the middle of area 41. A significant difference is observed between layer V and the other layers. (E) Effects of 10 μM CNQX, an antagonist of non-NMDA glutamate receptors, on the long inter-areal propagation recorded in area 20 and elicited by stimulation of various layers in area 41. The amplitudes of the responses in the presence of CNQX were normalized by those before the application (CTL). (F) Effects of cutting the white matter at the site of the areal boundary. The amplitudes of the responses after cutting were normalized by those before cutting (CTL).

synapses. Cutting the white matter under the areal boundary had almost no effect on the propagation of the neural activities ($n=8$; Fig. 4F), indicating that the activity propagation between the sites of stimulation and recording was mostly conveyed via local connections in the gray matter, although there is a possibility that the axons that make connections between different sites of areas 41 and 20 may travel through the white matter.

Activity-dependent potentiation of Ca²⁺ responses in the pathways from the primary to the secondary auditory cortices

Previously, we found activity-dependent potentiation of Ca²⁺ responses propagating between the primary auditory cortex and

dorsal area 18a in the presence of 1 μM bicuculline (Hishida et al., 2003). Similar potentiation of polysynaptic activities was found in layer V pyramidal neurons of area 41 after low-frequency stimulation (Kitaura et al., 2004). Here, we investigated the potentiation of Ca²⁺ responses induced by low-frequency stimulation in the presence of 1 μM bicuculline in slices including ventral area 20. Test stimulation with a single pulse at 100 μA was applied to layer V of area 41 in slices loaded with rhod-2 and perfused with 1 μM bicuculline. Initially, a Ca²⁺ rise observed in area 41 did not clearly invade area 20 (Fig. 5A). After application of conditioning stimulation at 300 μA to the same site at 12 s intervals for 10 min, the Ca²⁺ rise elicited by the test stimulation spread into the region including the entire areas 41 and 20 (Fig. 5B) in all 8 slices tested. The
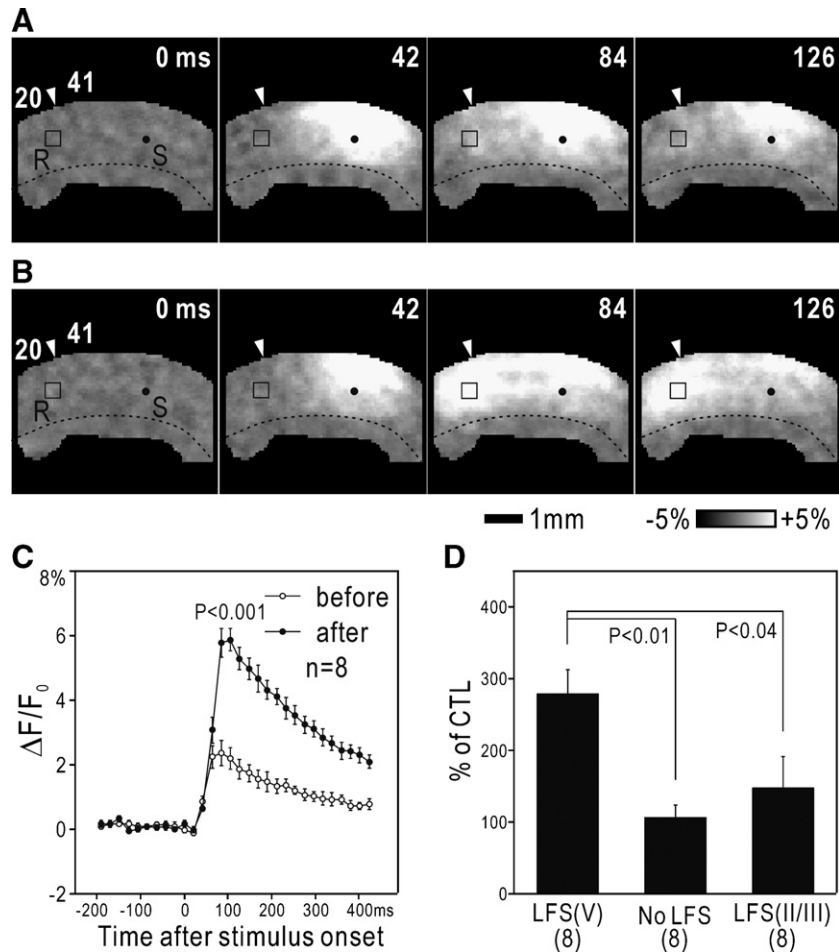
Fig. 5. Potentiation of Ca^{2+} responses propagating from the primary auditory cortex to ventral area 20. (A) Polysynaptic activities visualized as a Ca^{2+} rise elicited by test stimulation with a single pulse at 100 µA applied to layer V in area 41 (S and black dots, 2 mm apart from the boundary) in the presence of 1 µM bicuculline. (B) Ca^{2+} response elicited by test stimulation after conditioning stimulation (repetitive stimulation at 12 s intervals for 10 min, 300 µA). (C) Time courses of the Ca^{2+} signal in the windows (squares) in panels A and B (layer V, 500 apart µm from the boundary). A significant difference is found between the maximal amplitudes recorded 84 ms after the stimulus onset. (D) Normalized amplitudes of potentiation with or without conditioning stimulation (LFS) applied to layer V or layer II/III.

amplitude of the Ca^{2+} signal was measured in layer V of area 20 at the boundary, and significantly increased from $2.4 \pm 0.4\%$ to $5.8 \pm 0.5\%$ ($n=8$, $P<0.001$; Fig. 5C). The potentiation induced by conditioning stimulation of layer V ($279 \pm 34\%$, $n=8$) was significantly larger than the changes without stimulation ($106 \pm 17\%$, $n=8$, $P<0.01$; Fig. 5D). Conditioning stimulation of layer II/III induced potentiation in only 2 of 8 slices tested, resulting in significantly less marked potentiation ($148 \pm 43\%$, $n=8$, $P<0.04$; Fig. 5D).

Next, we investigated the properties of other connections surrounding the primary auditory cortex using Ca^{2+} imaging. When the conditioning stimulation was applied to layer V of area 20, no significant potentiation was observed (Fig. 6Ab). The activity propagation from the primary auditory cortex to caudal area 36 was significantly increased from $1.8 \pm 0.4\%$ to $5.9 \pm 1.1\%$ according

to the $\Delta F/F_0$ changes ($P<0.03$), while no clear potentiation was induced in the reverse direction (Figs. 6Ac, d). Other pathways between areas 41 and 18a (Figs. 6Ae, f) and between areas 41 and 39 (Figs. 6Ag, h) exhibited no significant potentiation (Fig. 6B). Taken together, the conditioning stimulation induced significant potentiation of Ca^{2+} responses in the pathways from the primary to the secondary auditory cortices, while no such potentiation was clearly observed in other pathways surrounding the primary auditory cortex.

Different critical periods of the bidirectional connections between the primary auditory cortex to ventral area 20

Sound experiences in young animals influence the development of the auditory cortex (Zhang et al., 2002). It is also expected that

Fig. 6. Potentiation of Ca^{2+} responses in the pathways between the primary auditory cortex and surrounding areas. (A) Potentiation of Ca^{2+} responses in various areas. The activities were elicited by test stimulation with a single pulse at 100 µA applied to layer V (S and black dots) in the presence of 1 µM bicuculline. The responses before and after conditioning stimulation (repetitive stimulation at 12 s intervals for 10 min, 300 µA) are shown. In the center schematic drawing, the sizes of the arrows give a rough impression of the magnitudes of the potentiation. (B) Comparison of the amplitudes of the Ca^{2+} responses propagating via the areal boundaries. The responses were evaluated in the windows (squares) shown in panel A. (For further description, see legend to Fig. 5. The choice of stimulation and recording sites was described in Materials and methods.)
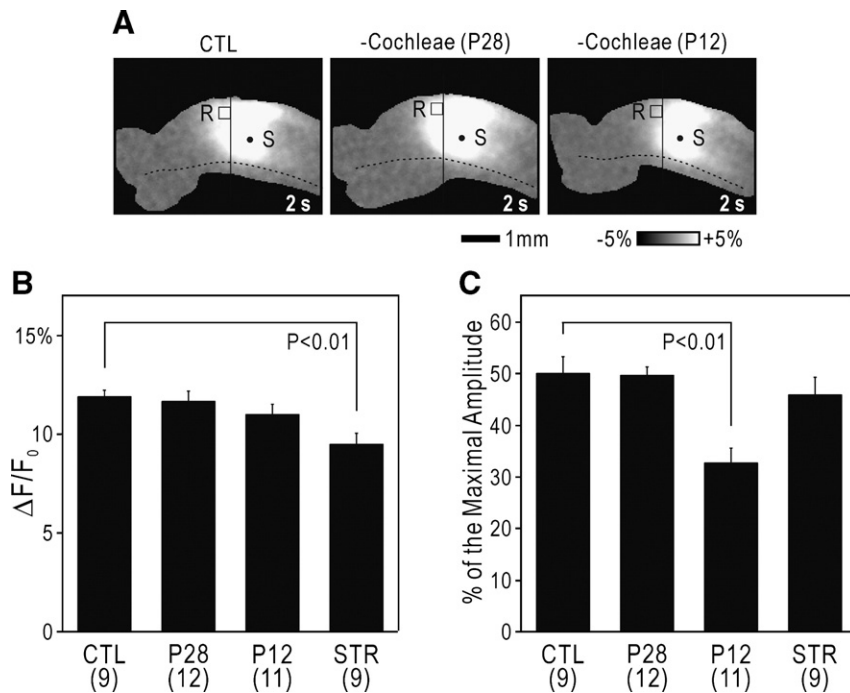
A

B
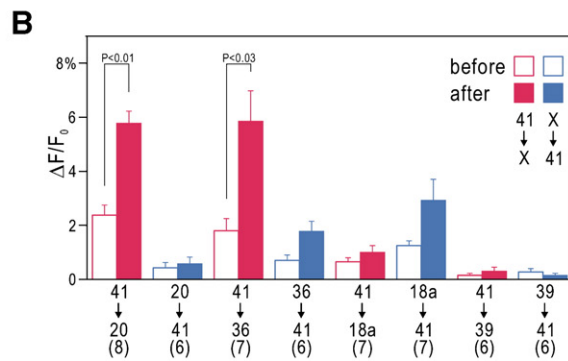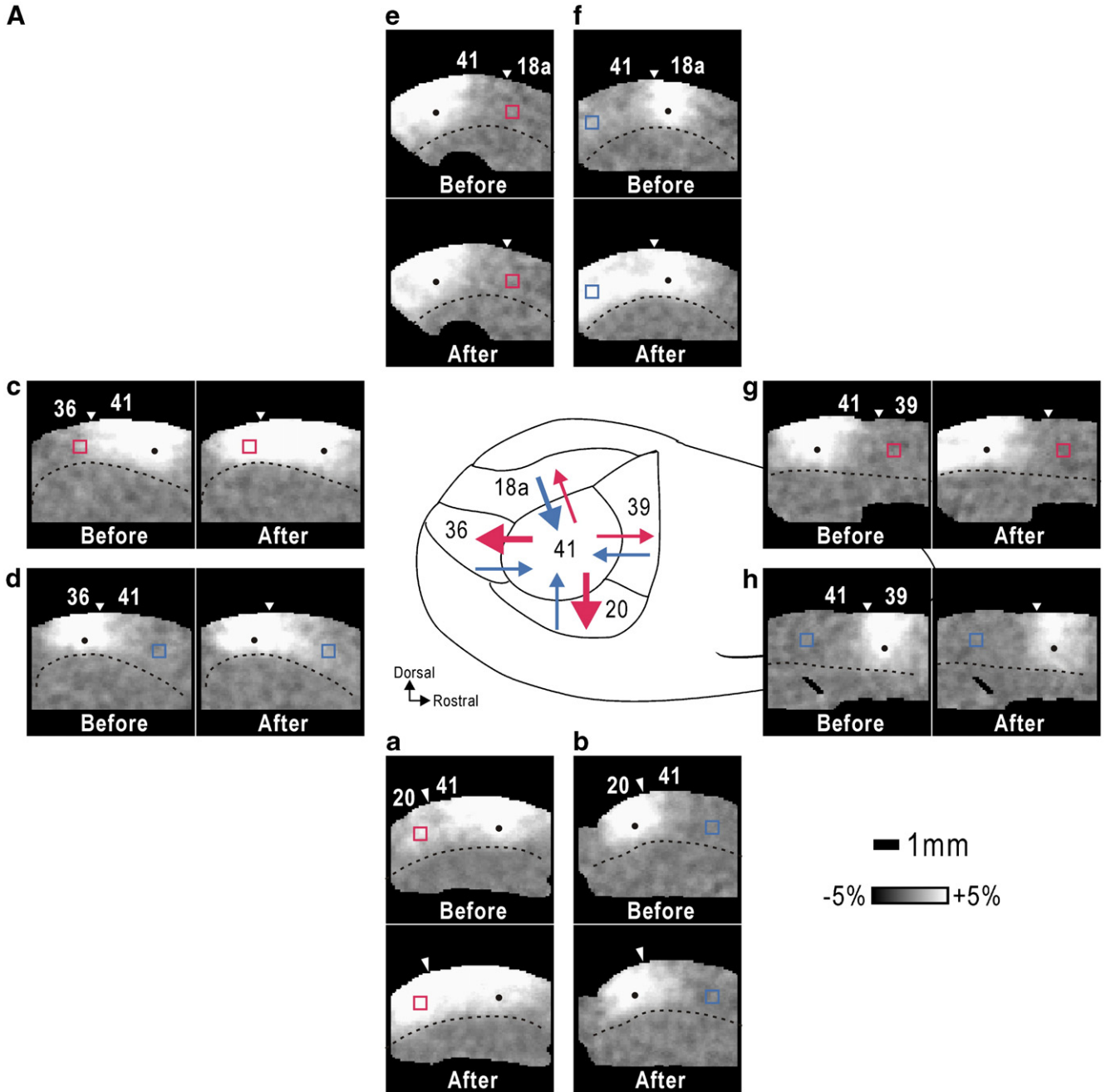
Fig. 7. Effects of bilateral cochlear lesions on activity propagation from the primary auditory cortex to ventral area 20. (A) Flavoprotein fluorescence responses elicited by repetitive stimulation (200 μA, 10 Hz for 1 s) of layer V in area 41 (500 μm from the areal boundary). (B) Maximal amplitudes of the fluorescence responses measured at 2 s after the stimulus onset. STR refers to the results in rats treated with streptomycin. (C) Activity propagation from area 41 to area 20. The amplitudes of the responses in the recording windows (squares) at 2 s were normalized by the maximal amplitudes shown in panel B. The windows were placed in layer II/III of area 20 adjacent to the boundary, as shown in panel A. (For further description, see legend to Fig. 2.)
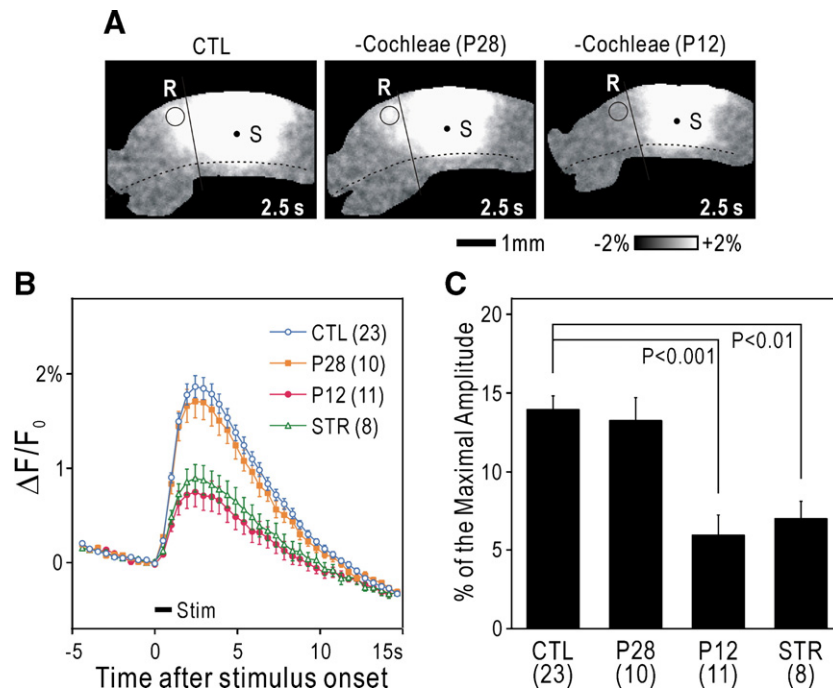

Fig. 8. Long inter-areal activity propagation from the primary auditory cortex to ventral area 20 affected by bilateral cochlear lesions. (A) Flavoprotein fluorescence responses elicited by repetitive stimulation (200 μA, 10 Hz for 1 s). Weak activities are emphasized in the images. (B) Time courses of the fluorescence changes in the circular windows in panel A. (C) Activity propagation from area 41 to area 20 measured at 2.5 s after the stimulus onset. The amplitudes of the responses in the windows were normalized by the maximal amplitudes of the fluorescence responses measured at 2.5 s. (For further description, see legend to Fig. 4.)

sound experiences have an effect on the functional connections between the primary auditory cortex and surrounding areas. To test this possibility, both cochleae were lesioned mechanically at P10–12 or P28 or by application of streptomycin from P10 to P28, and slices were prepared from the rats at 7 weeks of age or later (Fig. 7). First, the amplitudes of the flavoprotein fluorescence responses elicited by layer V stimulation in area 41 were measured (Fig. 7A). The maximal amplitude was slightly, but significantly, reduced in the rats treated with streptomycin compared with the control rats ($P < 0.01$, Fig. 7B). We further investigated the activity propagation from the primary auditory cortex to ventral area 20 (Fig. 7C), and found that it was significantly reduced by the cochlear lesions at P10–12 ($P < 0.01$).

We also investigated the long inter-areal (>1 mm) activity propagation from the primary auditory cortex to ventral area 20. This parameter was significantly reduced by the cochlear lesions at P10–12 or treatment with streptomycin ($P < 0.001$ and $P < 0.01$, respectively; Figs. 8A–C), while no apparent effect was observed in rats with cochlear lesions at P28. These findings strongly suggest that the development of functional connections from the primary auditory cortex to ventral area 20 was facilitated by cochlear inputs between P10 and P28.

The effects of cochlear lesions on the functional connections from ventral area 20 to the primary auditory cortex were investigated (Fig. 9). The maximal amplitude of the fluorescence responses in area 20 was slightly, but significantly, reduced not only by the cochlear lesions at P10–12 or treatment with streptomycin but also by the cochlear lesions at P28 compared with that in control rats ($P < 0.001$, $P < 0.001$ and $P < 0.02$, respectively; Figs. 9A, B). The activity propagation from area 20 to the primary auditory cortex was significantly reduced in the rats with cochlear lesions at P28

($P < 0.04$) and P10–12 ($P < 0.01$) or treatment with streptomycin ($P < 0.01$; Fig. 9C). These results strongly suggest that the development of functional connections from area 20 to the primary auditory cortex was facilitated by cochlear inputs even after P28.

Discussion

Flavoprotein fluorescence imaging in slices

In this study, we visualized and quantified the neural activities that propagate via the boundaries between the primary auditory cortex and surrounding areas using flavoprotein fluorescence imaging. This imaging can detect not only the neural responses elicited by electrical stimulation (Shibuki et al., 2003; Murakami et al., 2004; this study), but also the neural responses elicited by natural stimuli and their cortical plasticities (Shibuki et al., 2006; Takahashi et al., 2006). These studies demonstrate that flavoprotein imaging reflects functional activity, and not that it can only be detected after electrical activation of massive, coherently active inputs. This imaging method has several technical merits. First, flavoprotein fluorescence imaging does not necessitate the use of exogenous dyes, such that artificial effects of the dyes or damage caused by the staining (Yasuda and Tsumoto, 1996) can be avoided. In our previous study (Hishida et al., 2003), 1 μM bicuculline was required to elicit polysynaptic activities propagating via the areal boundary. However, polysynaptic activities were elicited by repetitive stimulation in the absence of bicuculline in the present study. It has been suggested that flavoprotein signals mostly reflect the polysynaptic activities produced by glutamatergic transmission (Kamatani et al., 2004). Second, the experimental
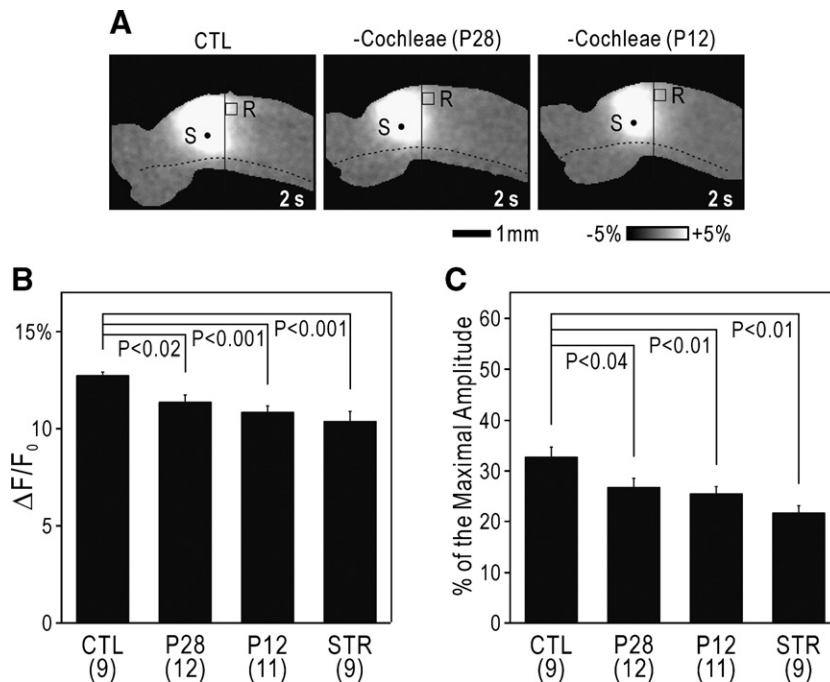

Fig. 9. Effects of bilateral cochlear lesions on activity propagation from ventral area 20 to the primary auditory cortex. (A) Flavoprotein fluorescence responses elicited by repetitive stimulation (200 μA, 10 Hz for 1 s) of layer V in area 20 (500 μm from the areal boundary). (B) Maximal amplitudes of the fluorescence responses measured at 2 s after the stimulus onset. (C) Activity propagation from area 20 to area 41. The amplitudes of the responses in the recording windows (squares) at 2 s were normalized by the maximal amplitudes shown in panel B. The windows were placed in layer II/III of area 41 adjacent to the boundary, as shown in panel A. (For further description, see legend to Fig. 2.)

results obtained with flavoprotein imaging are more reproducible than those obtained with methods involving extrinsic indicator dyes, in which variable staining of slices sometimes produced variations in the results (data not shown). Third, flavoprotein fluorescence signals are very stable compared to those of indicator dyes (Shibuki et al., 2003). Forth, flavoprotein fluorescence signals can be measured by using the non-harmful level of excitation light. These merits of flavoprotein fluorescence imaging enabled us to quantitatively investigate weak activities, such as long inter-areal activity propagation from the primary auditory cortex to ventral area 20.

Functional connections between the primary auditory cortex and surrounding areas

We investigated functional connections between areas which are considered as the primary or secondary sensory areas. But in the absence of direct anatomical evidences which show hierarchical relationships between these areas, so it might be appropriate that the areas we investigated are referred to as the primary or non-primary areas. In this paper we use the terms "feedforward" and "feedback" as the word which simply indicates directions "from the primary to non-primary" and "from non-primary to the primary" areas, respectively.

We think that the visualized activities are produced not only by the inter-areal circuits but also local circuits within the cortex. We investigated and compared the properties of the different functional connections by visualizing the polysynaptic activities. The imaging methods we used, especially flavoprotein imaging, have slow time resolutions, so the visualized connections were polysynaptic feedforward/feedback connections. These connections contain not only the circuits which directly connect one area to another (monosynaptic feedforward/feedback connections), but also the polysynaptic local circuits around areal boundaries which convey information collectively in a direction from one area to another. So it is possible that polysynaptic feedforward/feedback connections may share some common properties with monosynaptic ones and may show some different properties which might be caused by the polysynaptic local circuits (later for further discussion). It is also possible that the evoked polysynaptic feedforward/feedback activities which were observed in this study may be caused only by the activities of the polysynaptic local circuits without the involvements of the monosynaptic feedforward/feedback connections. In this study, we didn't investigate the cortical circuits in detail, but we have succeeded to obtain an overall view of neural propagation conveyed via the areal boundaries surrounding the primary auditory cortex.

We investigated the properties of activity propagation produced by repetitive electrical stimulation. It cannot be ruled out with this technique that axons from distant areas are passing through the stimulation site on their way to the site where most imaged activity is located. In our previous study (Hishida et al., 2003), supragranular field potentials were elicited by single pulse stimulation applied to layer V. In this experiment, local application of ibotenic acid to the stimulated site mostly suppressed local activities in layer V, while supragranular field potentials remained intact. This result suggests that the supragranular field potentials elicited by single pulse stimulation could be produced by antidromic activation of neurons in the recording site or activation of passing fibers. However, flavoprotein fluorescence responses elicited by single pulse stimulation were observed only in restricted areas (data not shown), indicating that activity propagation observed

after repetitive stimulation was mainly produced by polysynaptic activities. Intracellular recordings in supragranular pyramidal neurons during repetitive stimulation of remote areas also supported this conclusion (Kamatani et al., 2004).

The present study was performed based on a classical anatomical organization of the cerebral cortex (Krieg, 1946a,b). Previously, we have reported that myeloarchitecture can be observed in a fresh slices because of light-scattering properties of myelinated fibers (Hishida et al., 2003). Thus identified cortical areas are generally well correlated to those in the classical map developed by Krieg, since fine differences in myeloarchitecture were used for identification of cortical areas in this classical map. Although modern cortical maps (for example, a map developed by Zilles and Wree) may be better for classifying cortical areas (Zilles and Wree, 1985), the information obtained from fresh slices is not sufficient for identifying cortical areas of modern maps. However, there is naturally an intimate relationship between the classical map developed by Krieg and the modern cortical maps (Zilles and Wree, 1985). Recently many functional subdivisions have been found in the rat auditory cortex (Doron et al., 2002; Kalatsky et al., 2005; Donishi et al., 2006). Our results may be applied to the areas including these functional subdivisions.

In this study, we defined the primary auditory cortex (area 41) as the region of the temporal cortex with a high density of thalamocortical myelinated fibers in translucent images of slices (Krieg, 1946a; Zilles and Wree, 1985; Hishida et al., 2003). These myelinated fibers are more densely distributed in peripheral regions of area 41 than in the central region (Zilles and Wree, 1985), suggesting that the structural heterogeneity of area 41 in rats may reflect functional subdivisions (Horikawa et al., 1988; Sally and Kelly, 1988; Doron et al., 2002; Rutkowski et al., 2003; Kalatsky et al., 2005). Consistent with this idea, cochlear lesions before P28 reduced the responsiveness of the ventral part of area 41, while only mild effects were found in the central part (data not shown). Therefore, it may be more appropriate to apply the heterogeneity of activity propagation found in the present study to pathways between one of the functional subdivisions of the primary auditory cortex and surrounding areas locating near the boundary of area 41.

The auditory areas of the rat cerebral cortex are composed of a core cortex (area 41) and a belt cortex (areas 20 and 36) (Patterson, 1977; Cipolloni and Peters, 1979). Flavoprotein fluorescence imaging and Ca^{2+} imaging revealed that the neural activities in area 41 tended to propagate or potentiate from the core cortex (primary) to the belt cortex (secondary). Electrophysiological recordings *in vivo* have also revealed that sound stimuli produce neural activities not only in area 41 but also in ventral area 20 and caudal area 36 (Barth et al., 1995; Sukov and Barth, 1998). Neural activities in surrounding areas can be explained by the auditory information mediated by the thalamocortical projections to these areas (Vaughan, 1983). However, our results indicate that a part of these activities may be mediated by inter-areal lateral connections in the gray matter. What is the role of the auditory inputs? It has been reported that intra-areal lateral connections have roles in cortical plasticity, such as induction of LTP in the auditory cortex (Kudoh and Shibuki, 1997), remapping in the somatosensory cortex (Hickmott and Merzenich, 2002), reorganization in the cat visual cortex (Gilbert, 1996) and spectral tuning in the cat auditory cortex (Read et al., 2001). If the inter-areal lateral connections have properties similar to these intra-areal ones, neural activity propagations from the primary cortex to the secondary auditory

cortex may function in plastic changes involving the primary auditory cortex and surrounding higher areas.

Dorsal area 18a, rostral area 39 and caudal area 36 may function in multisensory integration (Barth et al., 1995; Brett-Green et al., 2003, 2004). In this study, inter-areal lateral connections between area 41 and area 39 were weak and did not show any potentiation. However, functional connections from area 18a to area 41 showed potentiation in Ca^{2+} imaging, although the changes were not statistically significant. These findings are consistent with our previous report that this pathway exhibited marked potentiation under different experimental conditions (Hishida et al., 2003). Area 18a has been shown to be subdivided into several distinct areas (Coogan and Burkhalter, 1993), and the region of area 18a in the slices we used in this study seem to overlap area LM (lateromedial), gathered from their positions. Area LM and the primary visual cortex (area 17) are mutually connected anatomically (Domenici et al., 1995; Johnson and Burkhalter, 1996) and functionally (Shao and Burkhalter, 1996; Tropea et al., 1999). Auditory–visual evoked potentials have been recorded in area 18a probably corresponding to area LM (Barth et al., 1995). So, areas 41 and 17 may link via area LM, and these connections may function in audio-visual sensory integration. Auditory–visual evoked potentials have been also recorded in area 36 (Barth et al., 1995). Area 36 seem to overlap dorsal part of Te2 (Zilles and Wree, 1985), gathered from their positions. Te2 has been reported to be on the visual pathways to amygdala involved in fear conditioning and receive both auditory and visual inputs (Vaudano et al., 1991; Shi and Cassell, 1997; Shi and Davis, 2001). So, the functional connections from area 41 to area 36 which showed potentiation in Ca^{2+} imaging may also have a role in audio-visual sensory integration.

Mechanisms for unidirectional activity propagation and potentiation of Ca^{2+} responses between the primary and secondary auditory cortices

Anisotropic activity propagation between the primary and secondary auditory cortices may be produced by skewed distributions of lateral connections. It has been reported that 70% of synaptic connections between pairs of layer V pyramidal neurons in the somatosensory cortex are unidirectional (Markram et al., 1997). Many neuronal pairs connected with the same unidirectional connectivity may determine the dominant direction of activity propagation as a whole. A pair of neurons connected with a unidirectional connection may be produced according to the Hebbian rule from a bidirectionally connected neuronal pair, when the two neurons fire many times with a fixed time difference. Such a condition may be satisfied by a pair consisting of a neuron in the primary auditory cortex and a neuron in the secondary auditory cortex, since the latency of auditory-evoked potentials in the primary auditory cortex is shorter than that in the secondary auditory cortex (Di and Barth, 1992; Brett et al., 1994). A second possibility is that recurrent excitatory connections between pyramidal neurons in each area may produce anisotropic activity propagation. In our previous study, the amplitudes of monosynaptic EPSPs recorded in neurons in the secondary somatosensory cortex (S2) after stimulation of the primary somatosensory cortex (S1) were slightly larger than those recorded in S1 after S2 stimulation, while the amplitudes of polysynaptic EPSPs in S2 after S1 stimulation were much larger than those in S1 after S2 stimulation (Kamatani et al., 2004). This difference between the

monosynaptic and polysynaptic EPSPs can be explained if the excitatory inputs from S1 terminate in a group of S2 neurons that are intimately connected with recurrent excitatory connections, while the excitatory inputs from S2 terminate in S1 neurons that are only loosely connected with each other (Kamatani et al., 2004). Intimate recurrent connections between pyramidal neurons in S2 may be formed as a result of simultaneous firing of S2 neurons driven by common inputs from S1. This idea is also applicable to connections between the primary and secondary auditory cortices. Both mechanisms for producing unidirectional activity propagation require activity-dependence of the synaptic changes, consistent with the present finding that sensory deprivation of auditory inputs before P28 reduced activity propagation from the primary auditory cortex to ventral area 20.

In this study, significant potentiation of Ca^{2+} responses was found for polysynaptic feedforward pathways from the primary and secondary auditory pathways, which also exhibited dominant activity propagation in flavoprotein fluorescence imaging. The absence of Ca^{2+} responses in area 20 after stimulation and the requirement of conditioning stimulation of area 41 to evoke a rise of Ca^{2+} responses in area 20 may indicate the Ca^{2+} responses may be the product of the activities of not only monosynaptic feedforward pathway but also the polysynaptic local circuits around the areal boundary. If so, the polysynaptic local circuits may have a function in the plastic change of polysynaptic feedforward pathway. This potentiation of Ca^{2+} responses probably reflects potentiation of polysynaptic EPSPs in layer V pyramidal neurons, since both can be produced in the presence of 1 μM bicuculline by low-frequency stimulation of layer V (Kitaura et al., 2004). In the absence of bicuculline, layer V pyramidal neurons failed to exhibit potentiation after low-frequency stimulation, while bursting activities elicited by 5 stimulus pulses at 30 ms intervals were sufficient to induce potentiation (Kitaura et al., 2004). The latter type of potentiation induced without bicuculline is expected to be required for producing dominant activity propagation from the primary to the secondary auditory cortices.

Experience-dependent plasticity in functional connections between the primary auditory cortex and ventral area 20

The primary sensory cortices are influenced by deprivation of sensory information during their critical periods (Hubel and Wiesel, 1970; Buonomano and Merzenich, 1998; Heynen et al., 2003). Therefore, we investigated the effects of cochlear lesions. It is possible that area 41 and all the sensory cortices surrounding area 41 may be influenced by the cochlear lesions, since neurons responding to auditory stimuli are widely distributed in these areas (Wallace et al., 2004). In the present study, we focused on areas 41 and 20, since the boundary and functional connections between the two were clearly observed. Furthermore, we tested the possibility that these functional connections could be modified in an activity-dependent manner, since it has been shown that the inter-areal connections in the mouse visual exhibit experience-dependent plasticity (Dong et al., 2004b). Cochlear lesions at P10–12, but not P28, reduced polysynaptic feedforward activity propagation from the primary auditory cortex to ventral area 20. The critical period for polysynaptic feedforward connections may be comparable to that for tonotopic map plasticity in the rat primary auditory cortex (Zhang et al., 2001, 2002). In the mouse visual cortex, feedforward and feedback connections differ in their development and experience-dependence in the critical period (Dong et al.,

2004b). Similarly, polysynaptic feedback activity propagation from ventral area 20 to the primary auditory cortex was reduced by cochlear lesions at P28.

What are the roles of plasticity in the polysynaptic feedback connections? Higher sensory cortical areas are expected to influence information processing in the primary areas via feedback connections (Gilbert, 1996; Martinez-Conde et al., 1999; Larkum et al., 2004; Dong et al., 2004a), depending on the context, experience or attention (Braun et al., 2002; Durif et al., 2003; Murray et al., 2004). Area 20 in rats and the ventral secondary auditory cortex in mice are thought to be involved in auditory memory recognition in familiarity discrimination (Wan et al., 2001; Geissler and Ehret, 2004). Therefore, polysynaptic feedback connections from ventral area 20 to the primary auditory cortex may modulate information processing in area 41 depending on auditory memory. The plasticity maintained after P28 in this pathway may be required for proper adjustment of auditory information processing according to acoustic environments that may be altered by the reproduction process or seasonal variation.

Acknowledgments

References

Bai, W.Z., Ishida, M., Arimatsu, Y., 2004. Chemically defined feedback connections from infragranular layers of sensory association cortices in the rat. Neuroscience 123, 257–267.

Barth, D.S., Goldberg, N., Brett, B., Di, S., 1995. The spatiotemporal organization of auditory, visual, and auditory–visual evoked potentials in rat cortex. Brain Res. 678, 177–190.

Braun, C., Haug, M., Wiech, K., Birbaumer, N., Elbert, T., Roberts, L.E., 2002. Functional organization of primary somatosensory cortex depends on the focus of attention. NeuroImage 17, 1451–1458.

Brett, B., Di, S., Watkins, L., Barth, D.S., 1994. A horseradish peroxidase study of parallel thalamocortical projections responsible for the generation of mid-latency auditory-evoked potentials. Brain Res. 647, 65–75.

Brett-Green, B., Fifkova, E., Larue, D.T., Winer, J.A., Barth, D.S., 2003. A multisensory zone in rat parietotemporal cortex: intra- and extracellular physiology and thalamocortical connections. J. Comp. Neurol. 460, 223–237.

Brett-Green, B., Paulsen, M., Staba, R.J., Fifková, E., Barth, D.S., 2004. Two distinct regions of secondary somatosensory cortex in the rat: topographical organization and multisensory responses. J. Neurophysiol. 91, 1327–1336.

Buonomano, D.V., Merzenich, M.M., 1998. Cortical plasticity: from synapses to maps. Annu. Rev. Neurosci. 21, 149–186.

Calvert, G.A., Bullmore, E.T., Brammer, M.J., Campbell, R., Williams, S.C., McGuire, P.K., Woodruff, P.W., Iversen, S.D., David, A.S., 1997. Activation of auditory cortex during silent lipreading. Science 276, 593–596.

Cipolloni, P.B., Peters, A., 1979. The bilaminar and banded distribution of the callosal terminals in the posterior neocortex of the rat. Brain Res. 176, 33–47.

Coogan, T.A., Burkhalter, A., 1993. Hierarchical organization of areas in rat visual cortex. J. Neurosci. 13, 3749–3772.

Coutinho, V., Mutoh, H., Knopfel, T., 2004. Functional topology of the mossy fibre-granule cell–Purkinje cell system revealed by imaging of intrinsic fluorescence in mouse cerebellum. Eur. J. Neurosci. 20, 740–748.

Das, A., Gilbert, C.D., 1995. Long-range horizontal connections and their role in cortical reorganization revealed by optical recording of cat primary visual cortex. Nature 375, 780–784.

Di, S., Barth, D.S., 1992. The functional anatomy of middle-latency auditory evoked potentials: thalamocortical connections. J. Neurophysiol. 68, 425–431.

Domenici, L., Harding, G.W., Burkhalter, A., 1995. Patterns of synaptic activity in forward and feedback pathways within rat visual cortex. J. Neurophysiol. 74, 2649–2664.

Dong, H., Shao, Z., Nerbonne, J.M., Burkhalter, A., 2004a. Differential depression of inhibitory synaptic responses in feedforward and feedback circuits between different areas of mouse visual cortex. J. Comp. Neurol. 475, 361–373.

Dong, H., Wang, Q., Valkova, K., Gonchar, Y., Burkhalter, A., 2004b. Experience-dependent development of feedforward and feedback circuits between lower and higher areas of mouse visual cortex. Vision Res. 44, 3389–3400.

Donishi, T., Kimura, A., Okamoto, K., Tamai, Y., 2006. "Ventral" area in the rat auditory cortex: a major auditory field connected with the dorsal division of the medial geniculate body. Neuroscience 141, 1553–1567.

Doron, N.N., Ledoux, J.E., Semple, M.N., 2002. Redefining the tonotopic core of rat auditory cortex: physiological evidence for a posterior field. J. Comp. Neurol. 453, 345–360.

Dronkers, N.F., Pinker, S., Damasio, A., 2000. Language and the Aphasias. In: Kandel, E.R., Schwartz, J.H., Jessell, T.M. (Eds.), Principles of Neural Science, McGraw-Hill, pp. 1169–1187.

Durif, C., Jouffrais, C., Rouiller, E.M., 2003. Single-unit responses in the auditory cortex of monkeys performing a conditional acousticomotor task. Exp. Brain Res. 153, 614–627.

Geissler, D.B., Ehret, G., 2004. Auditory perception vs. recognition: representation of complex communication sounds in the mouse auditory cortical fields. Eur. J. Neurosci. 19, 1027–1040.

Gilbert, C.D., 1992. Horizontal integration and cortical dynamics. Neuron 9, 1–13.

Gilbert, C.D., 1996. Plasticity in visual perception and physiology. Curr. Opin. Neurobiol. 6, 269–274.

Halpern, A.R., Zatorre, R.J., 1999. When that tune runs through your head: a PET investigation of auditory imagery for familiar melodies. Cereb Cortex 9, 697–704.

Heynen, A.J., Yoon, B.J., Liu, C.H., Chung, H.J., Huganir, R.L., Bear, M.F., 2003. Molecular mechanism for loss of visual cortical responsiveness following brief monocular deprivation. Nat. Neurosci. 6, 854–862.

Hickmott, P.W., Merzenich, M.M., 2002. Local circuit properties underlying cortical reorganization. J. Neurophysiol. 88, 1288–1301.

Hishida, R., Hoshino, K., Kudoh, M., Norita, M., Shibuki, K., 2003. Anisotropic functional connections between the auditory cortex and area 18a in rat cerebral slices. Neurosci. Res. 46, 171–182.

Hofstetter, K.M., Ehret, G., 1992. The auditory cortex of the mouse: connections of the ultrasonic field. J. Comp. Neurol. 323, 370–386.

Horikawa, J., Ito, S., Hosokawa, Y., Homma, T., Murata, K., 1988. Tonotopic representation in the rat auditory cortex. Proc. Jpn. Acad. 64, 260–263.

Hubel, D.H., Wiesel, T.N., 1970. The period of susceptibility to the physiological effects of unilateral eye closure in kittens. J. Physiol. 206, 419–436.

Illing, R.B., Cao, Q.L., Förster, C.R., Laszig, R., 1999. Auditory brainstem: development and plasticity of GAP-43 mRNA expression in the rat. J. Comp. Neurol. 412, 353–372.

Johnson, R.R., Burkhalter, A., 1996. Microcircuitry of forward and feedback connections within rat visual cortex. J. Comp. Neurol. 368, 383–398.

Burkhalter, R.R., 1997. A polysynaptic feedback circuit in rat visual cortex. J. Neurosci. 17, 7129–7140.

Kalatsky, V.A., Polley, D.B., Merzenich, M.M., Schreiner, C.E., Stryker, M.P., 2005. Fine functional organization of auditory cortex revealed

by Fourier optical imaging. Proc. Natl. Acad Sci. U. S. A. 102, 13325–13330.

Kamatani, D., Hishida, R., Kudoh, M., Shibuki, K., 2004. Functional connections between the primary and secondary somatosensory cortices in the rat slices visualized with autofluorescence imaging. Soc. Neurosci. 64213.

Kitaura, H., Hishida, R., Kudoh, M., Shibuki, K., 2004. Activity-dependent persisting modification of polysynaptic neural circuits involving layer V pyramidal neurons in rat auditory cortex in vitro. Eur. J. Neurosci. 19, 356–364.

Kosslyn, S.M., Pascual-Leone, A., Felician, O., Camposano, S., Keenan, J.P., Thompson, W.L., Ganis, G., Sukel, K.E., Alpert, N.M., 1999. The role of area 17 in visual imagery: convergent evidence from PET and rTMS. Science 284, 167–170.

Krieg, W.J., 1946a. Connections of the cerebral cortex. I. The albino rat. A. Topography of the cortical areas. J. Comp. Neurol. 84, 221–275.

Krieg, W.J., 1946b. Connections of the cerebral cortex. I. The albino rat. B. Structure of the cortical areas. J. Comp. Neurol. 84, 277–323.

Krieg, W.J., 1947. Connections of the cerebral cortex. I. The albino rat. C. Extrinsic connections. J. Comp. Neurol. 86, 267–394.

Kudoh, M., Shibuki, K., 1997. Importance of polysynaptic inputs and horizontal connectivity in the generation of tetanus-induced LTP in the rat auditory cortex. J. Neurosci. 17, 9458–9465.

Larkum, M.E., Senn, W., Lüscher, H.R., 2004. Top-down dendritic input increases the gain of layer 5 pyramidal neurons. Cereb. Cortex 14, 1059–1070.

Markram, H., Lübke, J., Frotscher, M., Roth, A., Sakmann, B., 1997. Physiology and anatomy of synaptic connections between thick tufted pyramidal neurones in the developing rat neocortex. J. Physiol. 500, 409–440.

Martinez-Conde, S., Cudeiro, J., Grieve, K.L., Rodriguez, R., Rivadulla, C., Acuña, C., 1999. Effects of feedback projections from area 18 layers 2/3 to area 17 layers 2/3 in the cat visual cortex. J. Neurophysiol. 82, 2667–2675.

Minta, A., Kao, J.P.Y., Tsien, R.Y., 1989. Fluorescent indicators for cytosolic calcium based on rhodamine and fluorescein chromophores. J. Biol. Chem. 264, 8171–8178.

Murakami, H., Kamatani, D., Hishida, R., Takao, T., Kudoh, M., Kawaguchi, T., Tanaka, R., Shibuki, K., 2004. Short-term plasticity visualized with flavoprotein autofluorescence in the somatosensory cortex of anaesthetized rats. Eur. J. Neurosci. 19, 1352–1360.

Murray, S.O., Schrater, P., Kersten, D., 2004. Perceptual grouping and the interactions between visual cortical areas. Neural Netw. 17, 695–705.

Patterson, H.A. 1997. An anterograde degeneration and retrograde axonal transport study of the cortical projections of the rat geniculate body. PhD Dissertation. Boston University.

Read, H.L., Winer, J.A., Schreiner, C.E., 2001. Modular organization of intrinsic connections associated with spectral tuning in cat auditory cortex. Proc. Natl. Acad Sci. U. S. A. 98, 8042–8047.

Reinert, K.C., Dunbar, R.L., Gao, W., Chen, G., Ebner, T.J., 2004. Flavoprotein autofluorescence imaging of neuronal activation in the cerebellar cortex in vivo. J. Neurophysiol. 92, 199–211.

Rutkowski, R.G., Miasnikov, A.A., Weinberger, N.M., 2003. Characterisation of multiple physiological fields within the anatomical core of rat auditory cortex. Hear. Res. 181, 116–130.

Sally, S.L., Kelly, J.B., 1988. Organization of auditory cortex in the albino rat: sound frequency. J. Neurophysiol. 59, 1627–1638.

Saper, C.B., Iversen, S., Frackowiak, R., 2000. Integration of sensory and motor function. In: Kandel, E.R., Schwartz, J.H., Jessell, TM. (Eds.), Principles of Neural Science, McGraw-Hill, pp. 349–380.

Schaeppi, U., Krinke, G., FitzGerald, R.E., Classen, W., 1991. Impaired tunnel-maze behavior in rats with sensory lesions: vestibular and auditory systems. Neurotoxicology 12, 445–454.

Seki, K., Kudoh, M., Shibuki, K., 1999. Long-term potentiation of Ca^{2+} signal in the rat auditory cortex. Neurosci. Res. 34, 187–197.

Seki, K., Kudoh, M., Shibuki, K., 2001. Sequence dependence of posttetanic potentiation after sequential heterosynaptic stimulation in the rat auditory cortex. J. Physiol. 533, 503–518.

Shao, Z., Burkhalter, A., 1996. Different balance of excitation and inhibition in forward and feedback circuits of rat visual cortex. J. Neurosci. 16, 7353–7365.

Shi, C.J., Cassell, M.D., 1997. Cortical, thalamic, and amygdaloid projections of rat temporal cortex. J. Comp. Neurol. 382, 153–175.

Shi, C., Davis, M., 2001. Visual pathways involved in fear conditioning measured with fear-potentiated startle: behavioral and anatomic studies. J. Neurosci. 21, 9844–9855.

Shibuki, K., Hishida, R., Murakami, H., Kudoh, M., Kawaguchi, T., Watanabe, M., Watanabe, S., Kouuchi, T., Tanaka, R., 2003. Dynamic imaging of somatosensory cortical activity in the rat visualized by flavoprotein autofluorescence. J. Physiol. 549, 919–927.

Shibuki, K., Hishida, R., Kitaura, H., Takahashi, K., Tohmi, M. in press. Coupling brain function and metabolism: autofluorescence imaging of neural activities by local changes in energy metabolism. In: Gibson, G. and Dienel, G. (Eds), Handbook of Neurochemistry and Molecular Neurobiology, vol.5, Neural Energy Utilization. Kluwer Academic/ Plenum Publishers, New York.

Shibuki, K., Ono, K., Hishida, R., Kudoh, M., 2006. Endogenous fluorescence imaging of somatosensory cortical activities after discrimination learning in rats. NeuroImage 30, 735–744.

Sukov, W., Barth, D.S., 1998. Three-dimensional analysis of spontaneous and thalamically evoked gamma oscillations in auditory cortex. J. Neurophysiol. 79, 2875–2884.

Takahashi, K., Hishida, R., Kubota, Y., Kudoh, M., Takahashi, S., Shibuki, K., 2006. Transcranial fluorescence imaging of auditory cortical plasticity regulated by acoustic environments in mice. Eur. J. Neurosci. 23, 1365–1376.

Tropea, D., Sermasi, E., Domenici, L., 1999. Synaptic plasticity of feedback connections in rat visual cortex. Brain Res. Dev. Brain Res. 118, 61–67.

Vaudano, E., Legg, C.R., Glickstein, M., 1991. Afferent and Efferent Connections of Temporal Association Cortex in the Rat: A Horseradish Peroxidase Study. Eur. J. Neurosci. 3, 317–330.

Vaughan, D.W., 1983. Thalamic and callosal connections of the rat auditory cortex. Brain Res. 260, 181–189.

Wallace, M.T., Ramachandran, R., Stein, B.E., 2004. A revised view of sensory cortical parcellation. Proc. Natl. Acad Sci. U. S. A. 101, 2167–2172.

Wan, H., Warburton, E.C., Kuœmierek, P., Aggleton, J.P., Kowalska, D.M., Brown, M.W., 2001. Fos imaging reveals differential neuronal activation of areas of rat temporal cortex by novel and familiar sounds. Eur. J. Neurosci. 14, 118–124.

Weber, B., Burger, C., Wyss, M.T., von Schulthess, G.K., Scheffold, F., Buck, A., 2004. Optical imaging of the spatiotemporal dynamics of cerebral blood flow and oxidative metabolism in the rat barrel cortex. Eur. J. Neurosci. 20, 2664–2670.

Yasuda, H., Tsumoto, T., 1996. Long-term depression in rat visual cortex is associated with a lower rise of postsynaptic calcium than long-term potentiation. Neurosci. Res. 24, 265–274.

Zhang, L.I., Bao, S., Merzenich, M.M., 2001. Persistent and specific influences of early acoustic environments on primary auditory cortex. Nat. Neurosci. 4, 1123–1130.

Zhang, L.I., Bao, S., Merzenich, M.M., 2002. Disruption of primary auditory cortex by synchronous auditory inputs during a critical period. Proc. Natl. Acad Sci. U. S. A. 99, 2309–2314.

Zilles, K., Wree, A., 1985. The rat nervous system, vol. 1. Academic Press, Sydney.